



**HAL**  
open science

**Nature of  $(C_5Me_5)_2Mo_2O_5$  in water–methanol at pH 0–14. On the existence of  $(C_5Me_5)MoO_2(OH)$  and  $(C_5Me_5)MoO_2+$ : a stopped-flow kinetic analysis**

Edmond Collange, Juan Garcia, Rinaldo Poli

► **To cite this version:**

Edmond Collange, Juan Garcia, Rinaldo Poli. Nature of  $(C_5Me_5)_2Mo_2O_5$  in water–methanol at pH 0–14. On the existence of  $(C_5Me_5)MoO_2(OH)$  and  $(C_5Me_5)MoO_2+$ : a stopped-flow kinetic analysis. *New Journal of Chemistry*, 2002, 26 (9), pp.1249-1256. 10.1039/B202106B . hal-03284240

**HAL Id: hal-03284240**

**<https://hal.science/hal-03284240>**

Submitted on 20 Jul 2021

**HAL** is a multi-disciplinary open access archive for the deposit and dissemination of scientific research documents, whether they are published or not. The documents may come from teaching and research institutions in France or abroad, or from public or private research centers.

L'archive ouverte pluridisciplinaire **HAL**, est destinée au dépôt et à la diffusion de documents scientifiques de niveau recherche, publiés ou non, émanant des établissements d'enseignement et de recherche français ou étrangers, des laboratoires publics ou privés.

**Nature of  $(C_5Me_5)_2Mo_2O_5$  in Water-Methanol at pH 0-14. On the Existence of  $(C_5Me_5)MoO_2(OH)$  and  $(C_5Me_5)MoO_2^+$ : a Stopped-Flow Kinetic Analysis.**

Edmond Collange, Juan A. Garcia<sup>†</sup> and Rinaldo Poli\*

*Laboratoire de Synthèse et d'Electrosynthèse Organométalliques, Université de Bourgogne, Faculté de Science Gabriel, 6 boulevard Gabriel, 21000 Dijon, France*

Correspondence to: Prof. Rinaldo Poli

Laboratoire de Synthèse et d'Electrosynthèse Organométalliques

Faculté des Sciences "Gabriel"

6, Boulevard Gabriel

21000 Dijon (France)

tel: +33-03.80.39.68.81

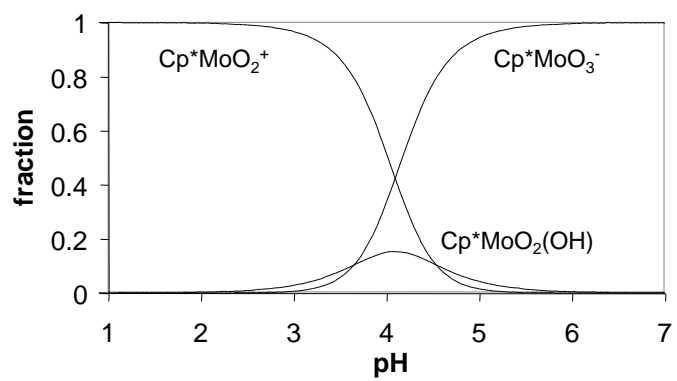
fax: +33-03.80.39.60.98

E-MAIL: [Rinaldo.Poli@u-bourgogne.fr](mailto:Rinaldo.Poli@u-bourgogne.fr)

---

<sup>†</sup> SOCRATES exchange student from the University of Zaragoza.

## Art work for table of contents



## Abstract.

A stopped-flow analysis of compound  $\text{Cp}^*\text{Mo}_2\text{O}_5$  ( $\text{Cp}^* = \eta^5\text{-C}_5\text{Me}_5$ ) in 20% MeOH-H<sub>2</sub>O in the pH range 0-14 has provided the speciation of this molecule as well as the rate and mechanism of interconversion between the various species that are present in solution. The compound is a strong electrolyte in this solvent combination, producing the  $\text{Cp}^*\text{MoO}_2^+$  and  $\text{Cp}^*\text{MoO}_3^-$  ions in equilibrium with a small amount of  $\text{Cp}^*\text{MoO}_2(\text{OH})$ , the latter attaining ca. 15% maximum relative amount at pH 4. At low pH (< 2.5)  $\text{Cp}^*\text{MoO}_2^+$  is essentially the only species present in solution, while the anion  $\text{Cp}^*\text{MoO}_3^-$  is the dominant species at pH > 6. The acid dissociation constant of  $\text{Cp}^*\text{MoO}_2(\text{OH})$  has been measured directly ( $\text{p}K = 3.65 \pm 0.02$ ) while the  $\text{p}K$  for the protonation equilibrium leading to  $\text{Cp}^*\text{MoO}_3\text{H}_2^+$  is estimated as < 0. The three trioxxygenated species establish rapid proton transfer equilibria among themselves, but transform to the dioxo species  $\text{Cp}^*\text{MoO}_2^+$  by two slower and independent first order pathways: loss of H<sub>2</sub>O from  $\text{Cp}^*\text{MoO}_3\text{H}_2^+$  and loss of OH<sup>-</sup> from  $\text{Cp}^*\text{MoO}_2(\text{OH})$ . The former pathway is prevalent at pH < 2, where the transformation proceeds to completion, giving rise to kinetics that are first order in metal and first order in [H<sup>+</sup>]. The reverse process is quantitative at pH > 5. The prevalent pathway at high pH is the addition of OH<sup>-</sup> to  $\text{Cp}^*\text{MoO}_2^+$ , giving rise to kinetics that are first order in metal and first order in [OH<sup>-</sup>]. The kinetics of the equilibration process at intermediate pH are affected by the buffer concentration, indicating a general acid/base catalytic phenomenon. The complete elucidation of the kinetic and thermodynamic scheme was made possible by the combined analyses of the equilibrium in the 3-5 pH range and the kinetics in the extreme pH regions.

## Introduction.

High oxidation state organometallic chemistry has experienced a rapid development in the last 20 years, mostly justified by the search for efficient oxidation catalysts. This is exemplified by the numerous studies carried out on the half-sandwich oxo derivatives of rhenium.<sup>1-3</sup> The coordination sphere of high oxidation state metals typically involves electronegative and  $\pi$ -donating ligands such as the halides or negatively charged oxygen-based (oxo, alkoxo) or nitrogen-based (nitrido, imido, amido) ligands. These conditions confer a high degree of covalency to any metal-carbon bond, which consequently becomes quite resistant to hydrolytic conditions. The cyclopentadienyl ligands are perhaps the most compatible organic fragments in this area of organometallic chemistry. It is therefore somewhat surprising that the physical behavior and chemical reactivity of high oxidation state organometallics is not systematically investigated in water, although some of these systems are synthesized in water or by the use of aqueous reagents.

Some of the earliest examples of high oxidation state organometallics are the molybdenum derivatives of general formula  $(\text{Ring})_2\text{Mo}_2\text{O}_5$  (Ring = substituted cyclopentadienyl ligand), first developed in the laboratory of M. L. H. Green for the parent cyclopentadienyl system.<sup>4-6</sup> We have recently reported improved syntheses of the Cp and Cp\* compounds (Cp =  $\eta^5\text{-C}_5\text{H}_5$ ; Cp\* =  $\eta^5\text{-C}_5\text{Me}_5$ ), and extended them to the preparation of new derivatives containing the sterically congested  $\text{C}_5\text{HPr}^i_4$  and  $1,2,4\text{-C}_5\text{H}_2\text{Bu}^t_3$  rings.<sup>7</sup> The structures of these compounds display neutral dinuclear units with symmetric Mo-( $\mu$ -O)-Mo bridges, like the various X-ray structures previously reported for different polymorphs of the Cp\* compound.<sup>8-11</sup> A related complex,  $\text{Cp}^*\text{MoO}_3^-$ , has been reported independently by Geoffroy and Sundermeyer.<sup>12-14</sup> These complexes can indeed be prepared in an aqueous medium,<sup>4, 7, 13-15</sup> but most reported investigations have been restricted to the use of non aqueous solvents.<sup>8-11, 16-19</sup>

We have initiated a research effort aimed at increasing our basic knowledge of the physical properties and chemical reactivity of organomolybdenum compounds in a variety of high oxidation states in water, with the goal in mind of developing new aqueous organometallic chemistry, catalysis and electrocatalysis. In this contribution, we report a thorough study of the Cp\*Mo<sup>VI</sup> system in an aqueous environment in the entire pH range (0-14). Since compound Cp\*<sub>2</sub>Mo<sub>2</sub>O<sub>5</sub> is insoluble in pure water, while alkali metal salts of Cp\*MoO<sub>3</sub><sup>-</sup> (e.g. sodium) are lipophobic, we were forced to carry out our investigation in a mixed MeOH-H<sub>2</sub>O solvent. However, the use of just 20% MeOH proved sufficient to keep the neutral compound in solution at sufficient concentrations (up to 4·10<sup>-4</sup> M) to carry out our UV-visible spectroscopic investigations, while it does not interfere with the aqueous chemistry of the Cp\*Mo<sup>VI</sup> species as shown by the results obtained.

### Experimental Section.

**Reagents and solutions.** All chemicals were of reagent grade and used as supplied without further purification. HNO<sub>3</sub> and NaOH standards solutions were from Merck-Prolabo normadoses. The buffers were constituted in single conjugate pairs or in Britton-Robinson (B.R.) mixtures.<sup>20, 21</sup> The ionic strength of all solutions was adjusted to 0.1 M by the addition of NaNO<sub>3</sub>. Compounds Cp\*<sub>2</sub>Mo<sub>2</sub>O<sub>5</sub> and Cp\*MoO<sub>2</sub>Cl were prepared according to the literature procedures.<sup>7</sup>

**pH and conductivity measurements.** The pH of the buffer solutions was determined, at 25 °C, with a Methrom 702 SM pHmeter. The electromotive force of the cell is expressed by the equation  $E = E_o - k(\text{pH}) + E_j$ .<sup>22</sup> In the presence of supporting electrolyte, such as 0.1 M NaNO<sub>3</sub>, the junction potential  $E_j$  is generally considered as constant in the pH range 2-12.<sup>23-25</sup> The above equation gives  $\text{pH} = (E_o - E)/k + E_j/k = \text{pH}_{\text{read}} + \Delta\text{pH}$ . The slope  $k$  ( $\approx 59$  mV) was obtained by calibration at 25 °C with NBS standard

buffers prepared in aqueous medium (0.05 M potassium biphthalate, pH = 4.008; 0.05 M borax, pH 9.196).<sup>26</sup> The correction term,  $\Delta\text{pH}$ , was determined daily by NaOH titration of a HNO<sub>3</sub> solution. It is the difference between the calculated and read pH values obtained in the acidic range. This term was generally close to -0.15 pH units. The  $\text{p}K_s$  of the mixed solvent (80:20 H<sub>2</sub>O-MeOH) is the sum of the experimental pH and the calculated pOH values in the basic range.<sup>27</sup> We have obtained  $\text{p}K_s = 14.25 \pm 0.02$ , close to the value determined by Rochester.<sup>25</sup> The electrical conductivity measurements were carried out with a YSI model 35 conductimeter and a Beckman 35 Conductivity Cell.

**Stopped-flow kinetic measurements.** The stopped flow kinetic runs were carried out with a Hitech SF-61-DX2 apparatus coupled with a Hitech diode-array UV-visible spectrophotometer. Kinetic traces were recorded at 25 °C in the pH range 1-13.25. The cell path length is 1 cm. Two types of manipulations were carried out as follows.

*Type 1 experiments (from Cp\*<sub>2</sub>Mo<sub>2</sub>O<sub>5</sub>).* A 2·10<sup>-3</sup> M Cp\*<sub>2</sub>Mo<sub>2</sub>O<sub>5</sub> stock solution was prepared in MeOH, since this compound is insoluble in water. For each stopped-flow kinetics run, the Cp\*<sub>2</sub>Mo<sub>2</sub>O<sub>5</sub> solution was prepared by diluting this stock solution with 4 volumes of H<sub>2</sub>O to obtain a 20:80 (v/v) solvent mixture. This operation was carried out no more than 1 min prior to injection into the stopped-flow cell. When the solution was allowed to stand for a long time (more than a half a day) at room temperature, the yellow starting compound reprecipitated. The above solution was mixed in the stopped-flow cell with an equivalent volume of a 20:80 (v/v) MeOH-H<sub>2</sub>O solution containing NaOH (for the kinetic run at pH ≥ 11.42) or a buffer at appropriate concentrations (see Results section) for the kinetic runs in the 7-10 pH region.

*Type 2 experiments (from Cp\*MoO<sub>3</sub><sup>-</sup>).* A 8·10<sup>-4</sup> M stock solution of Na<sup>+</sup>Cp\*MoO<sub>3</sub><sup>-</sup> in 20:80 (v/v) MeOH-H<sub>2</sub>O was prepared from the MeOH stock solution of Cp\*<sub>2</sub>Mo<sub>2</sub>O<sub>5</sub> by

dilution with 4 volumes of a diluted (ca.  $10^{-3}$  M) aqueous NaOH solution. This solution was mixed in the stopped-flow cell with an equivalent volume of a 20:80 (v/v) MeOH-H<sub>2</sub>O solution containing HNO<sub>3</sub> (for the kinetic runs at  $\text{pH} \leq 2.30$ ) or a buffer at appropriate concentrations (see Results section) for the kinetic runs in the 2.5-5 pH region.

**Data analysis.** All kinetic runs were analyzed with the program Specfit<sup>28</sup> while the fitting of the kinetic model to the observed first order rate constants and equilibrium constants as a function of pH (see Results) was carried out with the Excel Solver. The standard deviations on the determined parameters were obtained by means of the Solver Aid macro.<sup>29</sup>

## Results and Discussion

### (a) Kinetic study of the anation reaction of Cp\*<sub>2</sub>Mo<sub>2</sub>O<sub>5</sub>.

Solutions of Cp\*<sub>2</sub>Mo<sub>2</sub>O<sub>5</sub> in 20% MeOH-H<sub>2</sub>O are yellow and display an absorption spectrum which is characterized by a strong band in the UV with two shoulders at ca. 390 and 440 nm as shown by the trace *a* of Figure 1. The observed pH for this solution is ca. 4. This spectrum is qualitatively identical but has a lower intensity than that recorded on the same solution after lowering the pH to 1 by the addition of a strong acid (HNO<sub>3</sub>), see trace *b* of Figure 1. The reason of this phenomenon will become apparent after we have examined in detail the kinetics in the entire pH range (section d). When NaOH is added to the starting solution, on the other hand, this becomes essentially colorless, see trace *c* of Figure 1. The latter change is attributed to the formation of the previously described anion Cp\*MoO<sub>3</sub><sup>-</sup>.<sup>12-14</sup> This solution turns back yellow if, at this point, the pH is lowered again. The kinetics of this acidification process will be examined in detail in the next section. All



spectral changes witnessed during this investigation as a function of pH are perfectly reversible with no loss of intensity, indicating that all transformations are analytically clean.

<insert Figure 1>

The anation of  $\text{Cp}^*_2\text{Mo}_2\text{O}_5$  has been investigated by stopped-flow kinetics with UV-visible detection in the basic pH range by using NaOH solutions at different concentrations (pH 11.42-13.25) or buffers at pH < 11. In all cases, the final spectrum is identical to that shown in Figure 1 (c), showing that the transformation into the anionic complex  $\text{Cp}^*\text{MoO}_3^-$  proceeds to completion under these conditions. All transformations obey precise first order kinetics and the log of the observed rate constant ( $k_{\text{obs}}$ ) varies linearly with the pH (slope 1) for the pH > 11 data, as shown in Figure 2. This demonstrates that the slow step has a first order dependence on the concentration of  $\text{OH}^-$ . All  $k_{\text{obs}}$  values can be found in the Supporting Information. The behavior at pH < 11 will be analyzed in section h.

<insert Figure 2>

The rate law of this transformation could in principle be easily interpreted on the basis of a rate determining attack of  $\text{OH}^-$  to the dinuclear  $\text{Cp}^*_2\text{Mo}_2\text{O}_5$  complex, the nucleofuge being the  $\text{Cp}^*\text{MoO}_3^-$  anion. The resulting product of nucleophilic exchange, the conjugate acid  $\text{Cp}^*\text{MoO}_2(\text{OH})$ , would be immediately deprotonated under these pH conditions. The p*K* study of the  $\text{Cp}^*\text{MoO}_2(\text{OH})/\text{Cp}^*\text{MoO}_3^-$  couple, shown in the next section, confirms the validity of this statement. It will be shown later, however, that the given mechanistic interpretation is incorrect.

**(b) Protonation of  $\text{Cp}^*\text{MoO}_3^-$ : Formation of  $\text{Cp}^*\text{MoO}_2(\text{OH})$  and p*K* Study.**

A stock solution of  $\text{Cp}^*\text{MoO}_3^-$  in 20% MeOH-H<sub>2</sub>O was prepared by adding the minimum excess amount of NaOH to a  $\text{Cp}^*_2\text{Mo}_2\text{O}_5$  solution prepared as described above, in order to adjust the pH around 8-9. This was then mixed in the stopped-flow apparatus with various strong acid or buffer solutions, obtaining a final acidic pH. The UV-visible monitoring indicated the immediate change of the spectrum when the final pH was < 6, followed by a slower spectral evolution. We interpret this behavior as the result of an immediate protonation yielding  $\text{Cp}^*\text{MoO}_2(\text{OH})$  (proton transfer reactions are generally diffusion-controlled), which then evolves further. The implication of  $\text{Cp}^*\text{MoO}_2(\text{OH})$  during the protonation of  $\text{Cp}^*\text{MoO}_3^-$ , ultimately leading to the dinuclear complex  $\text{Cp}^*_2\text{Mo}_2\text{O}_5$ , has already been proposed but no spectroscopic evidence for the existence of this compound was reported.<sup>14</sup> Reactions of  $\text{Cp}^*\text{MoO}_3^-$  with other electrophiles  $\text{Y}^+$ , on the other hand, have allowed the isolation of stable  $\text{Cp}^*\text{MoO}_2(\text{OY})$  complexes, for instance with  $\text{Y} = \text{Si}(\text{CH}_2\text{Ph})_3$ .<sup>19</sup> The same transformation occurs for the tungsten analogue.

The  $pK$  value for the acid dissociation of  $\text{Cp}^*\text{MoO}_2(\text{OH})$  has been obtained from the analysis of the first spectrum (recorded within 1 ms from the time of mixing) as a function of pH, see Figure 3. The solutions buffered at  $\text{pH} > 6$  showed essentially the unaltered spectrum of  $\text{Cp}^*\text{MoO}_3^-$ , whereas the solutions buffered at  $\text{pH} < 2$  showed essentially the same spectrum, attributed to  $\text{Cp}^*\text{MoO}_2(\text{OH})$ . A SPECFIT<sup>28</sup> global analysis yields a  $pK = 3.65 \pm 0.02$  for the acid dissociation constant.

<insert Figure 3>

### **(c) Kinetic analysis of the $\text{Cp}^*\text{MoO}_2(\text{OH})$ evolution at $\text{pH} \leq 2$ .**

After the quantitative transformation of  $\text{Cp}^*\text{MoO}_3^-$  to its conjugate acid in the stopped-flow apparatus, the spectrum evolved ultimately yielding a pH independent final

spectrum (at  $\text{pH} < 2$ ), showing a quantitative transformation under these conditions. Figure 4 shows an example at  $\text{pH} 1$ . It is to be noted that this final spectrum (trace *b*) corresponds to trace *b* of Figure 1 and not to the spectrum of the starting  $\text{Cp}^*\text{Mo}_2\text{O}_5$  solution (trace *a* of Figure 1). Thus, the final product obtained from  $\text{Cp}^*\text{MoO}_2(\text{OH})$  under these conditions *is not the dinuclear species*.

<insert Figure 4>

All kinetics are first order in metal and give rise to the observed rate constants  $k_{\text{obs}}$  reported in the Supporting Information. These rate constants depend on the  $\text{pH}$  as shown in Figure 2. The slope of the  $\log k_{\text{obs}}$  vs.  $\text{pH}$  is  $-1$ , namely the reaction is first order with respect to  $[\text{H}^+]$ . On the basis of this observation, it is relative straightforward to propose that  $\text{Cp}^*\text{MoO}_2(\text{OH})$  undergoes a rapid and reversible protonation equilibrium to afford a  $\text{Cp}^*\text{MoO}_3\text{H}_2^+$  intermediate, which then decomposes in a slow rate determining step.

#### **(d) Kinetics in the equilibrium range.**

The above studies have shown that a quantitative conversion to  $\text{Cp}^*\text{MoO}_3^-$  occurs at  $\text{pH} > 7$  while a quantitative conversion to a new species occurs at  $\text{pH} \leq 2$ .<sup>30</sup> Adjusting the  $\text{pH}$  at intermediate values, starting from either a  $\text{Cp}^*\text{MoO}_3^-$  or a  $\text{Cp}^*\text{Mo}_2\text{O}_5$  solution, led to the evolution to a different and  $\text{pH}$ -dependent equilibrium situation. An example at  $\text{pH} 4.06$  is shown in Figure 5. Trace *a* is the first recorded spectrum starting from the  $\text{Cp}^*\text{MoO}_3^-$  solution and corresponds therefore to the acid dissociation equilibrium mixture of  $\text{Cp}^*\text{MoO}_3^-$  and  $\text{Cp}^*\text{MoO}_2(\text{OH})$ . This solution evolves toward the equilibrium solution (trace *c*) following *first order kinetics*. Trace *b* is the first recorded spectrum starting from the  $\text{Cp}^*\text{Mo}_2\text{O}_5$  solution (the true nature of which will be revealed in the next paragraph). This solution evolves to the *same* equilibrium solution (trace *c*), following again *first order*

*kinetics*. At each investigated pH value, starting from either solution yielded the *same equilibrium spectrum with identical observed first order rate constants* (within experimental error), provided that *the same buffer concentration* was used for both experiments, see section h. All individual values of the observed rate constants ( $k_{\text{obs}}$ ) can be found in the Supporting Information.

<insert Figure 5>

The results of the kinetics investigations in the equilibrium region demonstrate that compound  $\text{Cp}^*\text{Mo}_2\text{O}_5$  does not maintain its molecular, dinuclear nature in the 20% MeOH-H<sub>2</sub>O solution. Under the assumption that this species is indeed present and transforms to the anion by a first order process as seen in section (a), the microscopic reverse which becomes observable in the equilibrium region *should* have a second order dependence on the metal concentration. This situation occurs, for instance, for the equilibration between the mononuclear  $\text{HMoO}_3^+(\text{aq})$  and the dinuclear  $\text{H}_2\text{Mo}_2\text{O}_6^{2+}(\text{aq})$ .<sup>31</sup> However, this is not the case for our  $\text{Cp}^*\text{Mo}^{\text{VI}}$  system. This is further confirmed by the little or no dependence of the measured rate on the metal concentrations for the same pH value (data are available as Supporting Information). The strictly first order behavior observed *for all transformations at all pH values* forces us to conclude that only mononuclear species are involved.

**(e) Nature of the low pH species and nature of  $\text{Cp}^*\text{Mo}_2\text{O}_5$  in 20% MeOH-H<sub>2</sub>O.**

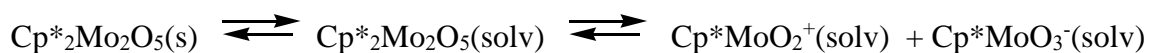
As seen above, the acidification of  $\text{Cp}^*\text{MoO}_3^-$  immediately affords  $\text{Cp}^*\text{MoO}_2(\text{OH})$  which decays (quantitatively at  $\text{pH} < 3$ ) to a new species with a rate law showing a first order dependence on the proton concentration. This behavior is interpreted as resulting from a fast and reversible protonation of  $\text{Cp}^*\text{MoO}_2(\text{OH})$  to afford a  $\text{Cp}^*\text{MoO}_3\text{H}_2^+$

intermediate, which then slowly evolves to a final product, now known to be mononuclear. It is straightforward to propose that the slow step correspond to dissociation of a water ligand, leading to the cationic complex  $\text{Cp}^*\text{MoO}_2^+$ , see Scheme 1,<sup>32</sup> which would therefore correspond to the dominant species at  $\text{pH} < 2$ . We shall now present further evidence confirming the presence of this cationic species before returning to the kinetic scheme.

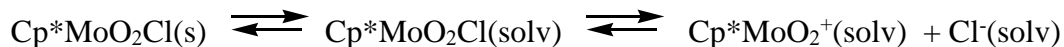
The implication of the above proposition and of Scheme 1 is that the dinuclear complex  $\text{Cp}^*_2\text{Mo}_2\text{O}_5$  ionizes in the 20% MeOH-H<sub>2</sub>O solution to initially produce a 1:1 mixture of the  $\text{Cp}^*\text{MoO}_2^+$  and  $\text{Cp}^*\text{MoO}_3^-$  ions, see Equation 1. Indeed, the spectrum of a  $\text{Cp}^*_2\text{Mo}_2\text{O}_5$  solution in Figure 1 (trace *a*) is quite close to a linear combination of the  $\text{Cp}^*\text{MoO}_2^+$  spectrum (trace *b*) and that of  $\text{Cp}^*\text{MoO}_3^-$  (trace *c*).<sup>33</sup> The ionic nature of  $\text{Cp}^*_2\text{Mo}_2\text{O}_5$  in 20% MeOH-H<sub>2</sub>O is confirmed by electrical conductivity studies, as shown in Figure 6. Under the validity of Equation 1, we wondered whether the known  $\text{Cp}^*\text{MoO}_2\text{Cl}$  complex would also ionize in the same medium (see Equation 2). The conductivity study of solutions of this compound fully confirm this hypothesis (Figure 6).

<insert Figure 6>

### Equation 1



### Equation 2



Although qualitatively quite convincing, the conductivity data present some unusual features from the quantitative point of view. The molar conductivity values vary more or less linearly with  $[\text{Cp}^*_2\text{Mo}_2\text{O}_5]^{1/2}$  or  $[\text{Cp}^*\text{MoO}_2\text{Cl}]^{1/2}$  for concentrations greater than  $4 \times 10^{-5}$

M, as expected for strong electrolytes. However, they are very large and the slopes of these lines are greater than expected for the low concentration range explored in our case (typical salts have an almost negligible variation in this range). Moreover, the linearity is lost for lower concentrations, and the molar conductivities at infinite dilutions are very large ( $> 300 \times 10^{-4} \text{ Ohm}^{-1} \text{ m}^2 \text{ mol}^{-1}$ ). Other 1:1 organic salts show conductivities in the range  $(80-115) \times 10^{-4} \text{ Ohm}^{-1} \text{ m}^2 \text{ mol}^{-1}$  in pure methanol for  $10^{-3} \text{ M}$  solutions.<sup>34</sup> Infinite dilution values are rarely above 150 for 1:1 salts except when hydronium ions are involved. All these features will in fact turn out to be completely consistent with our model. However, their full rationalization requires that we first detail the speciation of  $\text{Cp}^*\text{Mo}^{\text{VI}}$  in the entire pH range (section g).

Compound  $\text{Cp}^*_2\text{Mo}_2\text{O}_5$  is soluble in all common organic solvents and essentially insoluble in pure water. This indicates that the left hand side equilibrium of Equation 1 (dissolution of molecular  $\text{Cp}^*_2\text{Mo}_2\text{O}_5$ ) is highly sensitive to the hydrophobic nature of the molecule. However, the right hand side equilibrium of Equation 1 is highly sensitive to the dielectric constant. This view is confirmed by the comparison of the molar conductivities in different solvents at a  $4 \cdot 10^{-4} \text{ M}$  concentration, see Table 1. Thus, the water-rich solvent mixture used in this study favors an essentially complete ionization.

#### **(f) The complete scheme**

For convenience, the formulas of complexes  $\text{Cp}^*\text{MoO}_3^-$ ,  $\text{Cp}^*\text{MoO}_2(\text{OH})$  and  $\text{Cp}^*\text{MoO}_2^+$  will be heretofore abbreviated as  $\text{MoO}^-$ ,  $\text{MoOH}$  and  $\text{Mo}^+$ , respectively. The kinetic results described in sections (a) and (b) can now be reinterpreted according to Scheme 1, ultimately allowing us to understand and rationalize the kinetic and thermodynamic behavior of the  $\text{Cp}^*\text{Mo}$  system in the entire pH range. The vertical transformations on the right hand side of the scheme are simple protonation/deprotonation equilibria and are rapid (probably diffusion-limited) on the time scale of the stopped-flow

experiments. They can therefore be considered as a single species (abbreviated as *MO*, see Equation 3) for kinetic purposes. The kinetic evolution of the system under any pH condition can therefore be treated as a reversible first order equilibration between complex  $\text{Mo}^+$  on one side and the species *MO* (the intimate nature of which is pH dependent) on the other side. The development of the kinetic scheme affords Equation 4 for the overall rate constant of loss of oxygen-containing species (water and  $\text{OH}^-$ ) and Equation 5 for the overall rate of the uptake of oxygen-containing species. The observed rate constant ( $k_{\text{obs}}$ ) is then simply given as the sum of  $k_{+\text{obs}}$  and  $k_{-\text{obs}}$ . The  $k_{+\text{obs}}/k_{-\text{obs}}$  ratio, on the other hand, gives an operational equilibrium constant  $K_{\text{eq}}$  which will be pH dependent. This constant corresponds to the ratio between the sum of all oxygenated species (*MO*) and the non-oxygenated species  $\text{Mo}^+$ .

**Equation 3**

$$[MO] = [\text{MoO}^-] + [\text{MoOH}] + [\text{MoOH}_2^+]$$

**Equation 4**

$$k_{+\text{obs}} = \frac{k_{+1}K_s}{[\text{H}^+]} + k_{+2}$$

**Equation 5**

$$k_{-\text{obs}} = \frac{k_{-1} + \frac{k_{-2}[\text{H}^+]}{K_1}}{\frac{[\text{H}^+]}{K_1} + 1 + \frac{K_2}{[\text{H}^+]}}$$

On the basis of this scheme, it is now possible to see that the acidification of  $\text{MoO}^-$ / $\text{MoOH}$  leads to  $\text{Mo}^+$  by two different pathways, namely loss of  $\text{OH}^-$  from  $\text{MoOH}$  and loss

of water from  $\text{MoOH}_2^+$ , the latter predominating at low pH. The  $\text{p}K_2$  ( $3.65 \pm 0.02$ ) is available from the studies described in section (b), thus the term  $K_2/[\text{H}^+]$  in the denominator of Equation 5 is negligible at  $\text{pH} < 3$ . The protonation of MoOH does not occur to a significant extent down to  $\text{pH} 0$ . This is clearly shown by the study in Figure 2, provided that species  $\text{MoOH}_2^+$  would not have a spectrum perfectly identical to that of MoOH. This means that  $\text{p}K_1 \ll 0$  and the term  $[\text{H}^+]/K_1$  in the denominator of Equation 5 is also negligible. Under these conditions, Equation 5 simplifies to the rate law  $k_{\text{-obs}} = k_{-1} + (k_{-2}/K_1)[\text{H}^+]$ , or  $k_{\text{-obs}} = (k_{-2}/K_1)[\text{H}^+]$  when loss of water from species  $\text{MoOH}_2^+$  predominates, *i.e.* at low pH. Indeed, this is the observed trend. Since  $\text{p}K_1 < 0$ , individual values of  $k_{-2}$  and  $K_1$  cannot be obtained. Fitting the simplified rate law to the experimental data gives  $k_{-2}/K_1 = 17.26 \pm 0.22 \text{ s}^{-1}$ .

The reverse process (conversion of  $\text{Mo}^+$  to  $\text{MoOH}/\text{MoO}^-$ ) takes place by the microscopic reverse of the two pathways mentioned above, namely nucleophilic addition of either  $\text{H}_2\text{O}$  ( $k_{+2}$ ) or  $\text{OH}^-$  ( $k_{+1}$ ) to  $\text{Mo}^+$ . The expression of Equation 4 shows that the latter pathway will prevail at high pH giving rise to a first order dependence on  $[\text{OH}^-]$ , as experimentally observed. Fitting Equation 4 to the experimental data gives  $k_{+1} = (3.26 \pm 0.04) \times 10^3 \text{ s}^{-1}\text{L}$ . In order to elucidate the complete scheme, two rate constants are still missing:  $k_{-1}$  and  $k_{+2}$ . However, these are linked to each other by the thermodynamic cycle of Scheme 1, as shown by Equation 6. The operational equilibrium constant,  $K_{eq}$ , can therefore be expressed as in the simplified Equation 7, since  $\text{pH} > \text{p}K_1$  in all pH range (*vide supra*).

#### Equation 6

$$\frac{k_{+1}}{k_{-1}} K_s = \frac{k_{+2}}{k_{-2}} K_1$$

#### Equation 7



$$K_{eq} = \frac{k_{+1}K_s}{k_{-1} [H^+]} \left( 1 + \frac{K_2}{[H^+]} \right) = \frac{k_{+2} K_1}{k_{-2} [H^+]} \left( 1 + \frac{K_2}{[H^+]} \right)$$

In principle, the missing parameter may be obtained in two independent ways. The first one is via the rate of equilibration in the intermediate region and subsequent fitting of  $k_{obs}$  to the sum of Equation 4 and Equation 5. The second one is via the measurement of the pH-dependent equilibrium  $[MO]/[Mo^+]$  and fitting of Equation 7. The first method cannot be applied since the equilibration rates are affected by a general acid/base catalysis in the buffered pH region (*vide infra*). The second method is described in the next section.

### (g) The equilibrium in the intermediate pH range

The kinetic analyses in the extreme pH regions (< 2 and > 6) have provided us with the individual spectra of the pure species  $Mo^+$ ,  $MoOH$  and  $MoO^-$ , see above. We are therefore in a position to deconvolute the equilibrium spectrum obtained for the kinetic runs at each pH into the sum of the spectra of the above individual species. This operation is conveniently carried out with the program SPECFIT<sup>28</sup> and is facilitated by the independent knowledge of the  $[MoO^-]/[MoOH]$  ratio from the  $pK_2$  value. An excellent fit to the equilibrium spectrum was obtained at each pH value between 3 and 5. Outside this range, the equilibrium is too shifted to either side, *e.i.*  $Mo^+$  or the  $MoOH/MoO^-$  mixture ( $MO$ ), to obtain any meaningful information. The experimental values of the  $MO/[Mo^+]$  ratio are shown in Figure 2 together with the best fit given by Equation 7. It is to be noted that the  $K_{eq}$  curve has a transition from slope 1 to slope 2 in correspondence to the  $pK_2$  value. The fit of Equation 7 provides the individual values of  $k_{-1} = (6.32 \pm 0.03) \times 10^{-7} \text{ s}^{-1}$  and  $k_{+2} = (5.01 \pm 0.12) \times 10^{-4} \text{ s}^{-1}$ . At this point, feeding all known rate and acidity constants into Equation 4 and Equation 5 (the  $K_2/[H^+]$  term in the denominator of this equation is neglected) provides the calculated curves shown in Figure 2.

From all derived rate and acidity constants (summarized in Table 2), it is now possible to obtain the detailed speciation of the  $\text{Cp}^*\text{Mo}^{\text{VI}}$  system at all pH values. The relative proportion of  $\text{MO}$  and  $\text{Mo}^+$  is given by Equation 7 and the relative proportion of species  $\text{MoOH}$  and  $\text{MoO}^-$  is provided by the  $\text{p}K_2$  expression. Species  $\text{MoOH}_2^+$  can be neglected. The result is graphically shown in Figure 7. According to this result,  $\text{Mo}^+$  is essentially the only species in solution at  $\text{pH} < 2.5$  while the  $\text{MoO}^-$  is the dominant species at  $\text{pH} > 6$ . All species, including  $\text{MoOH}$ , are simultaneously present in the intermediate pH range. The maximum relative concentration of  $\text{MoOH}$  (ca. 15%) will be present at  $\text{pH} \cong 4$ .

<insert Figure 7>

It now becomes evident that, upon dissolution in 20%  $\text{MeOH-H}_2\text{O}$ ,  $\text{Cp}^*_2\text{Mo}_2\text{O}_5$  will provide equivalent amounts of  $\text{Mo}^+$  and  $\text{MoO}^-$  and a small amount of  $\text{MoOH}$ , while the pH will self-regulate around 4.0 by hydrolysis of part of the  $\text{Mo}^+$ , provided the solutions are sufficiently concentrated ( $> 10^{-3}$  M). For more diluted solutions, a greater proportion of  $\text{Mo}^+$  hydrolyzes to afford  $\text{MoO}^-$  and twice the same amount of protons. A similar behavior occurs when the  $\text{Mo}^+$  species is generated by the ionization of  $\text{Cp}^*\text{MoO}_2\text{Cl}$ . The concentrations of the different species  $\text{H}^+$ ,  $\text{OH}^-$ ,  $\text{Mo}^+$ ,  $\text{MoOH}$  and  $\text{MoO}^-$  can be calculated in a straightforward fashion from all known equilibrium constants. The results are presented in Figure 8 *a*, *b* and *c*.

<insert Figure 8>

At this point, we can analyze again and correctly interpret the results of the electrical conductivity study shown in Figure 6. In order to fit the conductivity data, the molar conductivities,  $\lambda_+$  or  $\lambda_-$  of every ionic species at each concentration were considered identical to the value  $\lambda_+^0$  or  $\lambda_-^0$  at infinite dilution. This is a reasonable hypothesis given

our small concentrations ( $<8 \times 10^{-4}$  M). In addition, the values of  $\lambda_{\text{H}^+}^0$  and  $\lambda_{\text{Cl}^-}^0$  were fixed to the literature values ( $228.8 \times 10^{-4}$  and  $48 \times 10^{-4}$  S.mol<sup>-3</sup>.m<sup>3</sup>, respectively)<sup>35</sup> as all attempts to keep them as free parameters led to instability. A global fitting of both Cp\*<sub>2</sub>MoO<sub>5</sub> and Cp\*MoO<sub>2</sub>Cl curves with common molar conductivities yielded a very good agreement between the experimental and calculated curves according to our kinetic and thermodynamic scheme (see Figure 9), the values of  $\lambda_{\text{Mo}^+}^0$  and  $\lambda_{\text{MoO}^-}^0$  provided by the fit being  $(72 \pm 6) \times 10^{-4}$  and  $(39 \pm 10) \times 10^{-4}$  S.mol<sup>-3</sup>.m<sup>3</sup>, respectively. These two values are in a reasonable range and are relatively close to each other, as one might expect from the similar size of the two ions. The determination of these values with a higher precision is prevented by the limited solubility of the compound and by the small contribution of these ions to the electrical conductivity at low concentrations in the presence of a significant amount of the more mobile protons.

<insert Figure 9>

#### **(h) The equilibration rate at intermediate pH: general acid/base catalysis.**

In order to provide an independent verification of the numerical values for all rate constants, kinetic analyses were also attempted in the intermediate pH region. This required the use of a variety of different buffer solutions, as detailed in the experimental section. Given the results outlined in the previous section, we were obviously expecting to obtain overall equilibration rate constants  $k_{\text{obs}}$  along the theoretical curve shown in Figure 2. As already mentioned, the transformations were found to follow perfect first order kinetics under all conditions, including the equilibrium region ( $2 < \text{pH} < 6$ ). However, the observed values of the first order rate constants turned out infallibly greater than expected. This phenomenon may be attributed to a general acid/base catalysis operated by the buffer's non-dissociated acid(s) and/or its(their) conjugate base(s). Hydrogen bonding

interactions between an undissociated acid and MoOH and MoOH<sub>2</sub><sup>+</sup> make the ligands OH<sup>-</sup> and H<sub>2</sub>O, respectively, better leaving groups, while the same kind of interactions between the buffer conjugate base and free water molecules or OH<sup>-</sup> ions make these better nucleophiles.

This state of affairs is unambiguously proven by detailed studies at different buffer concentrations while keeping the pH and metal concentration constant. Examples are shown in Figure 10. At each given pH value, the extrapolation of the rate constants to a zero buffer concentration should afford a value in agreement with our developed scheme. This expectation is indeed verified for the experiments at pH 7.97 (TRIS) and 9.24 (borax), see Figure 2. In other cases, on the other hand, the extrapolation to zero buffer concentration is not sufficiently precise, or the extrapolated value remains significantly higher than the value which is predicted by our scheme. The latter phenomenon occurs in particular within the pH range 2-6. We speculate that this may be caused by the presence of significant equilibrium amounts of compound Cp\*MoO<sub>2</sub>(OH), acting itself as a general acid/base catalyst.

<insert Figure 10>

### **(i) Nature of the MoOH<sub>2</sub><sup>+</sup> and Mo<sup>+</sup> species**

Two different tautomeric forms can be conceived for the Cp\*MoO<sub>3</sub>H<sub>2</sub><sup>+</sup> ion, namely an aquo-dioxo and a dihydroxo-oxo form, see **I** and **II**. Although the water elimination process requires transit through form **II**, the most stable species may be either one of these two forms. The precise proton distribution for many inorganic aqua ions of molybdenum does not seem to be established with certainty.<sup>36</sup> For instance, compound "MoO<sub>3</sub>" is often written as either Mo(OH)<sub>6</sub> or MoO<sub>2</sub>(OH)<sub>2</sub>(H<sub>2</sub>O)<sub>2</sub>. However, if we assume that all proton transfer processes are extremely fast, then the possible involvement of an equilibration

between the two tautomers would not affect the rate law of the overall transformation, no matter which of the two is the more stable species.

<insert **I** and **II**>

The nature of the  $\text{Mo}^+$  species also warrants a brief discussion. First, from a kinetic point of view, it would not be possible to distinguish between  $\text{Cp}^*\text{MoO}_2^+$  and an adduct containing a solvent molecule. This molecule, however, could not be  $\text{H}_2\text{O}$  since this would be obtained directly by protonation of  $\text{Cp}^*\text{MoO}_2(\text{OH})$  which, as argued earlier, should be an essentially diffusion-limited process. We should then consider the possibility that a  $\text{MeOH}$  molecule is coordinated to the  $\text{Mo}$  center. This possibility, however, is to be considered unlikely for the following reasons. This cationic species is present at a non negligible percentage in solution, in equilibrium with  $\text{Cp}^*\text{MoO}_2(\text{OH})$  and  $\text{Cp}^*\text{MoO}_3^-$ , up to ca. pH 5 (see Figure 7). Since the  $\text{p}K$  of  $\text{Cp}^*\text{MoO}_2(\text{OH}_2)^+$  ( $\text{p}K_1$ ) was estimated as  $< 0$  from kinetic evidence and since  $\text{MeOH}$  is only slightly less acidic than  $\text{H}_2\text{O}$  ( $\text{p}K_s = 15.5$ ), the  $\text{p}K$  of an hypothetical  $\text{Cp}^*\text{MoO}_2(\text{MeOH})^+$  species could not be much greater than 0. This is incompatible with the existence of this species up to pH 5. For these reasons, we believe that the low pH species is in fact a bare  $\text{Cp}^*\text{MoO}_2^+$  cation. It is to be remarked that when both terminal oxo ligands participate in  $\text{Mo-O}$  bonding with both their available  $\pi$  lone pairs (thereby giving rise to a formal  $\sigma+2\pi$  triple bond), the  $\text{Cp}^*\text{MoO}_2^+$  complex achieves a saturated, 18-electron configuration. The loss of bonding to the  $\text{H}_2\text{O}$  molecule would therefore be compensated at least partially by an increase of O-to-Mo  $\pi$  donation. Efforts to isolate a stable salt of this cationic complex and study its molecular and electronic structure are currently underway in our laboratory.

It is possible to find a parallel between the aqueous chemistry of  $\text{Cp}^*\text{Mo}^{\text{VI}}$  and that of inorganic molybdenum, when we notice that the  $(\text{Cp}^*)\text{Mo}$  unit is isoelectronic with the  $\text{Mo}(\text{H}_2\text{O})_3$  or with the  $\text{Mo}(\text{H}_2\text{O})_2(\text{OH}^-)$  unit. Thus, compound  $\text{Cp}^*_2\text{Mo}_2\text{O}_5$  has a parallel in

complex  $[\text{Mo}_2\text{O}_4(\mu\text{-O})(\text{H}_2\text{O})_6]^{2+}$ , while compound  $\text{Cp}^*\text{MoO}_2(\text{OH})$  has parallels in complexes  $\text{MoO}_2(\text{OH})(\text{H}_2\text{O})_3^+$  and  $\text{MoO}_2(\text{OH})_2(\text{H}_2\text{O})_2$ .<sup>36</sup> The "unsaturated" complex  $\text{Cp}^*\text{MoO}_2^+$  would be related to a species such as  $\text{MoO}_2(\text{OH})(\text{H}_2\text{O})_2^+$  or  $\text{MoO}_2(\text{H}_2\text{O})_3^{2+}$ . Like the proton distribution discussed above, the precise hydration level is often unclear for molybdenum aqua ions.<sup>36</sup> While aqueous "MoO<sub>3</sub>" is believed to adopt 6-coordination as mentioned above, its conjugate base is usually written as  $\text{HMoO}_4^-$  (this obviously referring to a 4-coordinate  $\text{MoO}_3(\text{OH})^-$  complex) and the corresponding dianion  $\text{MoO}_4^{2-}$  is believed to be 4-coordinate. Thus, the unsaturation of  $\text{Cp}^*\text{MoO}_2^+$  should not be considered surprising.

## Conclusions

The present investigation has uncovered the speciation of the  $\text{Cp}^*\text{Mo}^{\text{VI}}$  unit in the entire pH range in an essentially pure aqueous environment. The presence of 20% methanol is necessary to avoid the precipitation of neutral  $\text{Cp}^*_2\text{Mo}_2\text{O}_5$  but does not directly participate in the speciation equilibria. The study has revealed the existence and stability as a function of pH of the hitherto unreported complexes  $\text{Cp}^*\text{MoO}_2(\text{OH})$  and  $\text{Cp}^*\text{MoO}_2^+$ . In addition, the involvement of a complex having formula  $\text{Cp}^*\text{MoO}_3\text{H}_2^+$  as an intermediate in the generation of  $\text{Cp}^*\text{MoO}_2^+$  at low pH has been evidenced by the kinetic studies.

A parallel has been established between the aqueous behavior of  $\text{Cp}^*\text{Mo}^{\text{VI}}$  and inorganic  $\text{Mo}^{\text{VI}}$ . An important difference, however, is related to the inertness of the  $\text{Cp}^*\text{-Mo}$  bond, which resists hydrolysis down to pH 0. This has the consequence of blocking three coordination positions, rendering the  $\text{Cp}^*\text{Mo}^{\text{VI}}$  species unable to aggregate beyond the dinuclear level. Aqueous inorganic  $\text{Mo}^{\text{VI}}$ , on the other hand, forms a large variety of polyoxomolybdate ions in the pH range 2-5.<sup>36</sup> As a result, the speciation of  $\text{Cp}^*\text{Mo}^{\text{VI}}$  is relatively simple. The results presented in this contribution assist us in the interpretation of

the reductive chemistry and electrochemistry of Cp\*Mo<sup>VI</sup> in an aqueous environment, which is presented in another contribution.<sup>37</sup>

**Acknowledgement.** We are grateful to the Ministère de la Recherche and to the CNRS for general support through UMR 5632, and to the Conseil Régional de Bourgogne for providing part of the funds for the purchase of the stopped-flow apparatus.

## References

- 1 W. A. Herrmann, *Comments Inorg. Chem.*, 1988, **7**, 73-107.
- 2 W. A. Herrmann, *Angew. Chem., Int. Ed. Engl.*, 1988, **27**, 1297-1313.
- 3 W. A. Herrmann and F. E. Kühn, *Acc. Chem. Res.*, 1997, **30**, 169-180.
- 4 M. Cousins and M. L. H. Green, *J. Chem. Soc.*, 1964, 1567-1572.
- 5 M. Cousins and M. L. H. Green, *J. Chem. Soc. (A)*, 1969, 16-19.
- 6 M. J. Bunker and M. L. H. Green, *J. Chem. Soc., Dalton Trans.*, 1981, 847-851.
- 7 D. Saurenz, F. Demirhan, P. Richard, R. Poli and H. Sitzmann, *Eur. J. Inorg. Chem.*, in press.
- 8 P. Gomez-Sal, E. de Jesus, P. Royo, A. Vazquez de Miguel, S. Martinez-Carrera and S. Garcia-Blanco, *J. Organometal. Chem.*, 1988, **353**, 191-196.
- 9 J. W. Faller and Y. Ma, *J. Organometal. Chem.*, 1988, **340**, 59-69.
- 10 P. Leoni, M. Pasquali, L. Salsini, C. di Bugno, D. Braga and P. Sabatino, *J. Chem. Soc. Dalton Trans.*, 1989, 155-159.
- 11 A. L. Rheingold and J. R. Harper, *J. Organometal. Chem.*, 1991, **403**, 335-344.
- 12 M. S. Rau, C. M. Kretz, L. A. Mercado, G. L. Geoffroy and A. L. Rheingold, *J. Am. Chem. Soc.*, 1991, **113**, 7420-7421.

- 13 J. Sundermeyer, U. Radius and C. Burschka, *Chem. Ber.*, 1992, **125**, 2379-2384.
- 14 M. S. Rau, C. M. Kretz, G. L. Geoffroy and A. L. Rheingold, *Organometallics*, 1993, **12**, 3447-3460.
- 15 K. Umakoshi and K. Isobe, *J. Organometal. Chem.*, 1990, **395**, 47-53.
- 16 M. Herberhold, W. Kremnitz, A. Razavi, H. Schöllhorn and U. Thewalt, *Angew. Chem. Int. Ed. Engl.*, 1985, **24**, 601-602.
- 17 K. Isobe, S. Kimura and Y. Nakamura, *J. Organometal. Chem.*, 1987, **331**, 221-228.
- 18 F. Bottomley and J. Chen, *Organometallics*, 1992, **11**, 3404-3411.
- 19 M. S. Rau, C. M. Kretz, G. L. Geoffroy, A. L. Rheingold and B. S. Haggerty, *Organometallics*, 1994, **13**, 1624-1634.
- 20 M. A. Paul and F. A. Long, *Chem. Rev.*, 1957, **57**, 1-45.
- 21 The B.R. buffers were solutions of acetic, orthophosphoric, or boric acid partially neutralized with NaOH and containing NaNO<sub>3</sub>.
- 22 J. Costa, R. Delgado, M. G. B. Drew, V. Felix and A. Saint-Maurice, *J. Chem. Soc., Dalton Trans.*, 2000, 1907-1916.
- 23 R. G. Bates, 'Determination of pH: theory and practice', John Wiley & Sons, 1965.
- 24 E. Bosch, P. Bou, H. Allemann and M. Roses, *Anal. Chem.*, 1996, 3651-3657.
- 25 C. H. Rochester, *J. Chem. Soc., Dalton Trans.*, 1972, 5-8.
- 26 R. G. Bates, L. Johnson and R. A. Robinson, *Chem. Anal.*, 1972, **17**, 479-487.
- 27 A. Liberty and T. S. Light, *J. Chem. Educ.*, 1962, 236-239.
- 28 R. A. Binstead, B. Jung and A. D. Zuberbühler, 'Specfit/32', 2000 Spectrum Software Associates, 2000.
- 29 R. de Levie, *J. Chem. Educ.*, 1999, **76**, 1594-1598.



- 30 The formation of  $\text{Cp}^*\text{MoO}_3^-$  is in fact essentially quantitative at  $\text{pH} > 6$ , while the formation of the low pH species is essentially quantitative at  $\text{pH} < 3$ . The kinetics studies in sections (a) and (b) have been limited to  $\text{pH} > 9$  and  $< 2$ , respectively, for reasons that will become clear in section (g).
- 31 J. F. Ojo, R. S. Taylor and A. G. Sykes, *J. Chem. Soc. Dalton. Trans.*, 1975, 500-505.
- 32 The nomenclature for the rate constants has been chosen as follows: all  $k_+$  constants correspond to addition of oxygen species ( $\text{H}_2\text{O}$  or  $\text{OH}^-$ ), all  $k_-$  to loss of oxygen species; the subscript 1 corresponds to gain/loss of one proton, the subscript 2 to gain/loss of two protons.
- 33 The difference is attributable to the presence of a small amount of  $\text{Cp}^*\text{MoO}_2(\text{OH})$  at equilibrium, see section (h).
- 34 W. J. Geary, *Coord. Chem. Rev.*, 1971, **7**, 81-122.
- 35 Janz and Tomkins, 'Nonaqueous Electrolyte Handbook', Academic Press, 1972.
- 36 D. T. Richens, in 'Group 6 Elements: Chromium, Molybdenum and Tungsten', Chichester, 1997.
- 37 J. Gun, A. Modestov, O. Lev, D. Saurenz, M. Vorotyntsev and R. Poli, submitted for publication.

Table 1. Molar conductivities for  $4 \cdot 10^{-4}$  M solutions of  $\text{Cp}^*_2\text{Mo}_2\text{O}_5$  in different solvents.<sup>a</sup>

Solvent	$\Lambda/\text{Ohm}^{-1} \text{ m}^2 \text{ mol}^{-1}$
MeCN	0 <sup>b</sup>
$\text{CH}_2\text{Cl}_2$	0
EtOH	0.4
Acetone	0.8
MeOH	4.2
20% MeOH- $\text{H}_2\text{O}$	102

<sup>a</sup>Corrected for the molar conductivity of the pure solvent. <sup>b</sup>In this solvent, the measured conductivity was smaller for the solution than for the pure solvent.

Table 2. Summary of all rate and equilibrium constants (Scheme 1).

$\text{p}K_1$	$< 0$
$\text{p}K_2$	$3.65 \pm 0.02$
$k_{+1}$	$(3.26 \pm 0.04) \times 10^3 \text{ M}^{-1} \text{ s}^{-1}$
$k_{-1}$	$(6.32 \pm 0.03) \times 10^{-7} \text{ s}^{-1}$
$k_{+2}$	$(5.01 \pm 0.12) \times 10^{-4} \text{ s}^{-1}$
$k_{-2}/K_1$	$17.26 \pm 0.22 \text{ s}^{-1}$

## Captions for Figures

Figure 1. UV-visible spectra of 20% MeOH-H<sub>2</sub>O solutions of (a) pure Cp\*<sub>2</sub>Mo<sub>2</sub>O<sub>5</sub> (pH ca. 4); (b) Cp\*<sub>2</sub>Mo<sub>2</sub>O<sub>5</sub> after addition of HNO<sub>3</sub> (pH 1); (c) Cp\*<sub>2</sub>Mo<sub>2</sub>O<sub>5</sub> after addition of NaOH (pH = 11.42). All solutions have [Cp\*<sub>2</sub>Mo<sub>2</sub>O<sub>5</sub>] = 4·10<sup>-4</sup> M.

Figure 2. Plot of the experimental log *k*<sub>obs</sub> (triangles) and log *K*<sub>eq</sub> (squares) vs. pH. The curves drawn correspond to the best fit (*k*<sub>obs</sub>, *k*<sub>+obs</sub>, *k*<sub>-obs</sub> and *K*<sub>eq</sub>) according to the equations given in the Results section. Stars correspond to the *k*<sub>obs</sub> values extrapolated to zero buffer concentration. All solutions have [Cp\*<sub>2</sub>Mo<sub>2</sub>O<sub>5</sub>] = 4·10<sup>-4</sup> M.

Figure 3. Spectra in 20% MeOH-H<sub>2</sub>O of solution obtained by acidification of Cp\*MoO<sub>3</sub><sup>-</sup> at different pH values and recorded immediately (ca. 1 ms) after mixing. All initial solutions have [Cp\*MoO<sub>3</sub><sup>-</sup>] = 8·10<sup>-4</sup> M.

Figure 4. Key UV-visible spectra for the Cp\*MoO<sub>2</sub>(OH) evolution at pH 1 in 20% MeOH-H<sub>2</sub>O. (a) Initial spectrum (ca. 1 ms from mixing). (b) Final spectrum. (c) Spectrum of Cp\*MoO<sub>3</sub><sup>-</sup>. All initial solutions have [Cp\*MoO<sub>3</sub><sup>-</sup>] = 8·10<sup>-4</sup> M.

Figure 5. Key UV-visible spectra for the evolution of Cp\*MoO<sub>3</sub><sup>-</sup> and Cp\*<sub>2</sub>Mo<sub>2</sub>O<sub>5</sub> at pH 4.08 in 20% MeOH-H<sub>2</sub>O. (a) Initial spectrum from the Cp\*MoO<sub>3</sub><sup>-</sup> solution (ca. 1 ms from mixing). (b) Initial spectrum from the Cp\*<sub>2</sub>Mo<sub>2</sub>O<sub>5</sub> solution (ca. 1 ms

from mixing). (c) Equilibrium spectrum. (d) Reference spectrum at pH 11.35.  
(e) Reference spectrum at pH 1.

Figure 6. Molar conductivity of a 20% MeOH-H<sub>2</sub>O solution of Cp\*<sub>2</sub>Mo<sub>2</sub>O<sub>5</sub> (diamonds) or Cp\*MoO<sub>2</sub>Cl (triangles) as a function of concentration. The lines are a linear fit.

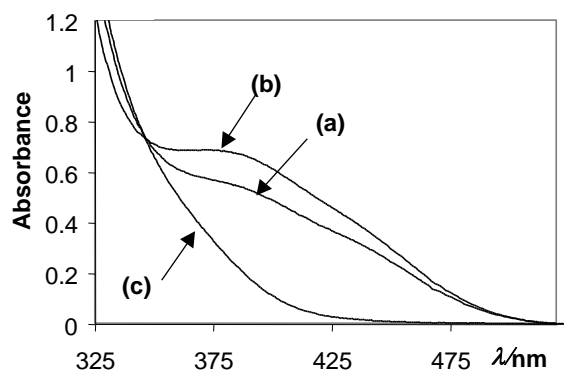
Figure 7. Relative proportion of species Mo<sup>+</sup>, MoOH and MoO<sup>-</sup> at all pH values in 20% MeOH-H<sub>2</sub>O.

Figure 8. (a) and (b): Calculated concentrations of H<sup>+</sup> (line only), Mo<sup>+</sup> (circles), MoO<sup>-</sup> (triangles) and MoOH (squares) for solutions of Cp\*<sub>2</sub>Mo<sub>2</sub>O<sub>5</sub> (8a) and Cp\*MoO<sub>2</sub>Cl (8b) in 20-80 MeOH-H<sub>2</sub>O. (c): Measured (squares: Cp\*<sub>2</sub>Mo<sub>2</sub>O<sub>5</sub>; triangles: Cp\*MoO<sub>2</sub>Cl) and calculated (lines) pH as a function of concentration.

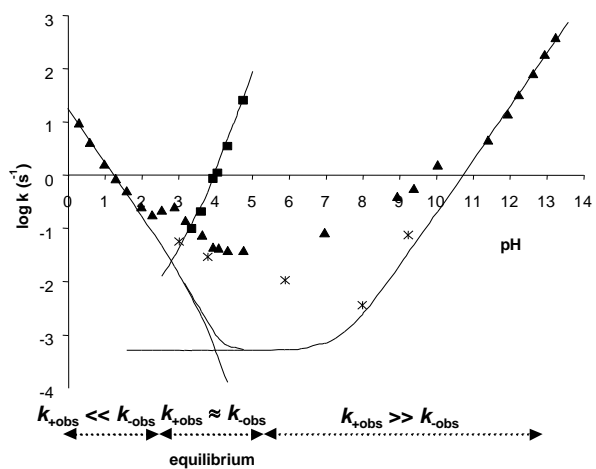
Figure 9. Measured and calculated conductivity in a 20:80 MeOH-H<sub>2</sub>O solution as function of the initial concentration for: Cp\*<sub>2</sub>Mo<sub>2</sub>O<sub>5</sub> (diamonds); Cp\*MoO<sub>2</sub>Cl (triangles).

Figure 10. First order equilibration constants  $k_{\text{obs}}$  as a function of buffer concentration at constant pH. Squares: TRIS (pH 7.97); diamonds : borax (pH 9.24); triangles: hydroxylamine (pH 6.34); +: chloroacetic (pH 3.01); circles: formic (pH 3.77); ×: acetic (pH 5.87).

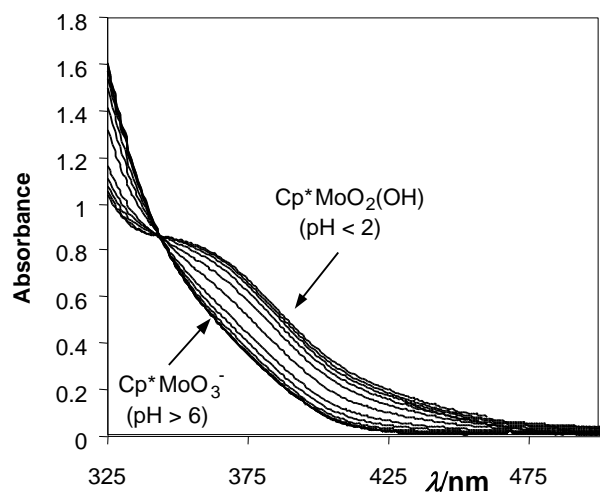
**Figure 1**



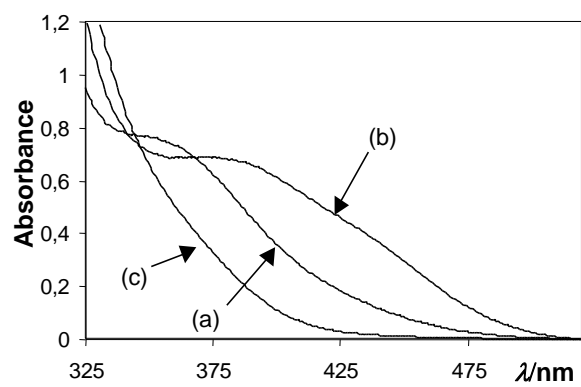
**Figure 2**



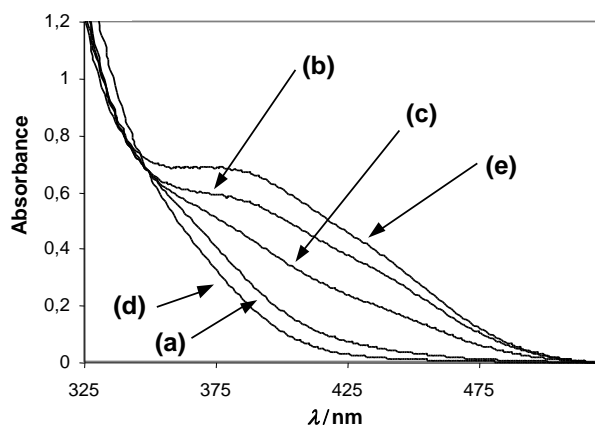
**Figure 3**



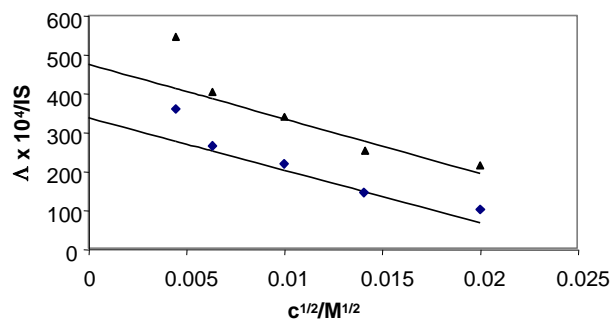
**Figure 4**



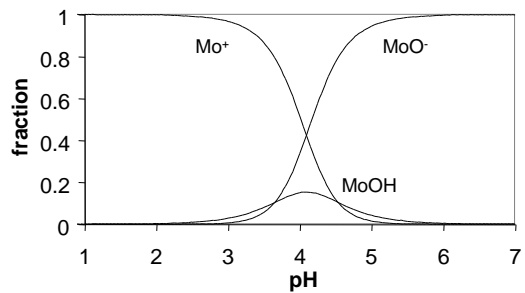
**Figure 5**



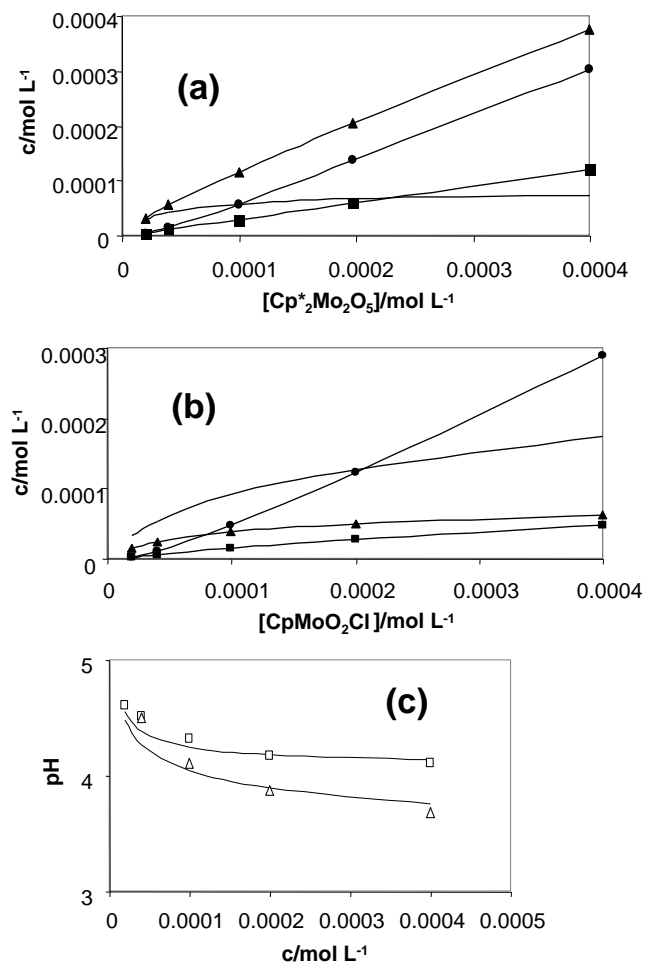
**Figure 6**



**Figure 7**

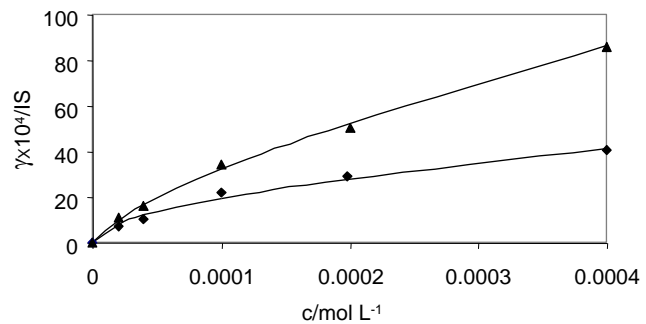


**Figure 8**

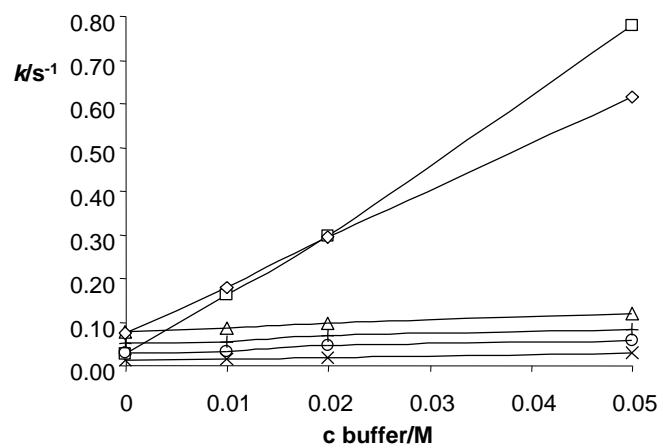


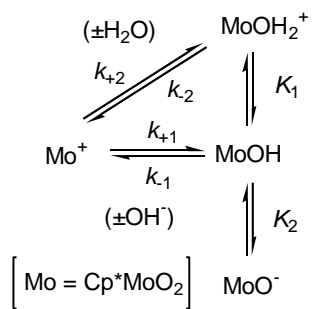


**Figure 9**



**Figure 10**





**Scheme 1**

